

## Diffusion of Barium in Barium Oxide\*

R. W. REDINGTON†

*Cornell University, Ithaca, New York*

(Received May 7, 1952)

The self-diffusion of barium in single crystals of barium oxide has been measured as a function of temperature in the range from 550°K to 1520°K. Two diffusion processes were found. Measurement of the ionic mobility (with a tracer technique) showed that one of these processes was charge-transporting ( $\sim 2$  electronic charges) and the other was not. At temperatures below 1350°K the diffusion was "structure sensitive" and could be affected by previous heat treatment. The temperature dependence for the non-charge-transporting diffusion was  $11 \pm 2.2$  ev above 1350°K and  $0.44 \pm 0.03$  ev below 1350°K. The corresponding figures for the charge-transporting diffusion were  $12 \pm 2.3$  ev and  $0.3 \pm 0.05$  ev. The surface diffusion constant for barium on barium oxide was also measured and had a temperature dependence of  $0.16 \pm 0.03$  ev.

### I. INTRODUCTION

THE purpose of this experiment was to measure the internal diffusion constant of barium in barium oxide and the surface diffusion constant as a function of temperature and to determine the charge transported by the diffusing barium. The effects of previous heat treatment on the internal diffusion were also investigated. The study was undertaken for two reasons: (1) quantitative information on the diffusion of barium as a function of temperature is desirable for the interpretation of thermionic experiments with BaO and for studies of its semiconducting properties; (2) diffusion studies on divalent ionic crystals should add to the understanding of ionic crystals, which at present is built largely on experiments on alkali halides.

### II. APPARATUS AND PROCEDURE

A radioactive tracer technique was used.<sup>1</sup> The tracer Ba was evaporated onto the surface of a crystal as BaO. After the crystal had been heated for some time the distribution of radioactive Ba in the crystal for the internal diffusion measurements was determined by sectioning the crystal with a microtome and measuring the activity of the sections; for the surface diffusion measurements a movable slit system was used to scan the distribution on the surface. The diffusion constants were calculated from these measured distributions.

The barium 140 used as the tracer was supplied by the Oak Ridge National Laboratories as BaCl in a weak acid solution. After the addition of about 0.1 mg carrier barium per millicurie of barium 140, the barium was precipitated as BaSO<sub>4</sub> and deposited in a small platinum evaporator cup in a centrifuge. This BaSO<sub>4</sub> was decomposed to the oxide by heating it to about 1100°K in the evaporator. The platinum cup was heated by a tungsten filament, and a platinum heat shield between the crystal sample and the platinum

cup exposed the crystal to only the interior of the cup. The temperature of a crystal under normal evaporating conditions was measured with a platinum-platinum 10 percent rhodium thermocouple imbedded in a test crystal. This temperature was only 130°C above room temperature. The usual evaporating time was about one hour and the diffusion during this time, as estimated from the extrapolation of the temperature dependence data to this temperature, was negligible in every case except one (a quenched crystal measurement). For that one case, a correction was made using the diffusion constant from the extrapolation. The pressure during the evaporation was less than  $10^{-5}$  mm of Hg.

The average dimensions of the crystal samples used were about  $3 \times 3 \times 1$  mm. The crystals for the internal diffusion measurements were mounted in a matrix of barium oxide. These crystal mounts were compressed from powdered barium oxide in a die with about  $10^4$  pounds/sq in. pressure. They were  $\frac{3}{8}$  in. in diameter and about  $\frac{1}{2}$  in. long, with a square face of the crystal exposed in one of the end faces. These mounts were sintered for about an hour at 1000°C. After this sintering operation and immediately before they were placed in the evaporator, the exposed crystal surface was ground and polished to present a fresh surface. This type of mount furnished a support during the heating of the crystal with a minimum of contamination and was much more convenient to mount in the microtome than the small crystals.

A sketch of the interior of the vacuum oven used to heat the crystals is shown in Fig. 1. It is shown with a crystal for an internal diffusion run in a crystal mount of sintered barium oxide. This oven was constructed on a male ground glass joint with a 4-lead press which could be sealed into the vacuum system. A second nickel heat shield was supported inside the vacuum system, and the portion of the oven shown in the figure fitted into this heat shield. The inner quartz tube was attached to the press and this tube supported the oven. The oven winding was a tungsten helix, and the current was supplied by a voltage regulating transformer. This temperature regulation was satisfactory as the largest

\* This work has received support from a Frederick Gardner Cottrell Grant by the Research Corporation and from the ONR.

† Now at the General Electric Research Laboratory, Schenectady, New York.

<sup>1</sup> The general method and procedure were similar to that used in many previous investigations of diffusion, e.g., Maphother, Crooks, and Maurer, *J. Chem. Phys.* **18**, 1231 (1950).

variation in temperature during a run was about 0.5 percent. The temperature was measured with a 0.007-in. platinum—platinum 10 percent rhodium thermocouple which had been calibrated against a 0.020-in. Leeds and Northrup platinum—platinum 13 percent rhodium thermocouple. The cold junctions were connected to a pair of copper leads waxed through two holes in the water-cooled press. This oven was modified by the addition of two platinum-rhodium electrodes for the ionic mobility measurements, and the modified oven was also used for the surface diffusion measurements.

For the internal diffusion and ionic mobility measurements, the surface of the crystal mount in which the crystal was exposed was removed by filing, and about  $\frac{1}{2}$  mm of the four exposed edges of the crystal was removed in this operation. This procedure should eliminate edge effects because  $\frac{1}{2}$  mm was large compared to the distances through which measurable diffusion took place.

A microtome was constructed to section the crystal using a standard microtome knife reground to a  $45^\circ$  edge. The crystal holder and advance screw were mounted on the end of a horizontal crank which made sliding contact with a steel way near the knife edge. This steel way and the vertical bearing of the crank determined the cutting plane. The crystals were mounted in a holder which fitted into a chuck on the crystal advance screw. This mounting was done in a jig which indexed against the surface of the crystal to be cut. The worst misalignment observed between the crystal surface and the cutting plane was about 0.005 radian. The variations in the thickness of the sections because of the tendency of the crystal to cleave rather than slice and because of the lack of rigidity of the blade were much more serious than the variations caused by alignment or by variations in the pitch of the advance screw. The material removed in a slice came off as a powder, part of which stuck to the knife blade and part of which fell onto a sample tray placed below the knife. The portion which stuck to the blade was collected with a damp "camel's hair" brush. The material was flushed from the brush with water onto the sample tray. The samples were evaporated to dryness, forming thin sources which could be conveniently counted.

The Geiger counter had a  $2.3 \text{ mg/cm}^2$  mica end window, slightly larger than 1 in. in diameter and was shielded with  $1\frac{1}{2}$  in. of lead. The sample trays, which were inverted aluminum culture dishes, fitted over a boss on a brass tray which could be placed in a rack with a choice of distances from the counter. This arrangement insured reproducible geometry for the counting operations. Because  $\text{Ba}^{140}$  has a radioactive daughter product, lanthanum 140, which is also a  $\beta, \gamma$ -emitter, it was necessary to measure the decay in activity of most of the samples to determine the amount of  $\text{Ba}^{140}$  that was present. This determination was quite easy as the 40-hour half-life of the  $\text{La}^{140}$  is appreciably shorter than the 12.8-day half-life of  $\text{Ba}^{140}$ .

For the surface diffusion measurements, a movable slit system with a  $\frac{1}{4}$ -mm resolving power was constructed on a tray which fitted into the counter rack. Underneath the slit, a small dry box with a cellophane window was constructed to hold the surface diffusion samples. A dry box was necessary as barium oxide reacts with the water vapor in the air. The slit itself was constructed in  $\frac{1}{4}$ -in. aluminum and could be moved above the crystal by a micrometer screw.

The crystals used were grown by Dash<sup>2</sup> from the vapor phase on magnesium oxide pseudoseeds. At the time of the low temperature diffusion constant measurements, there were no single crystals available that were large enough to be cleaved into several samples, and most of the data in that temperature range were taken on samples cleaved from a polycrystalline plate. Three measurements in this temperature range were made on samples cleaved from a single crystal. As the measurements on this single crystal and the polycrystalline plate were consistent, the points are not separately identified on the figures. The polycrystalline plate consisted of similarly oriented crystals, about 1 mm across. In the data on these polycrystalline samples, about 3 percent of the radioactive material was found deeper in the crystal than expected from the rest of the distribution. As this did not appear in the single-crystal samples, it was presumed to be caused by grain boundary diffusion and was treated as background. The rest of the data were taken on samples from single crystals which showed only a few small flaws when viewed under  $24\times$  magnification. All of the data on the effects of heat treatments were taken on samples cleaved from the same crystal, and all the low temperature ionic mobility measurements were taken on samples cleaved from a similar crystal.

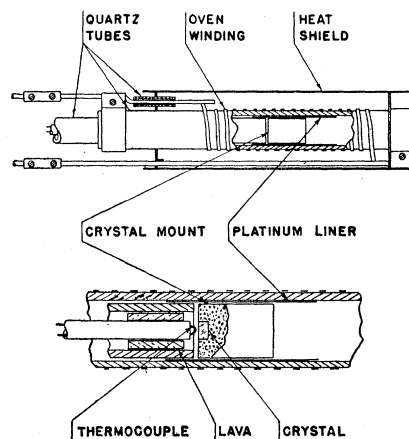


Fig. 1. Sketch of the vacuum oven. The upper figure shows the general arrangement of the oven and the lower figure shows an enlarged view of the immediate surroundings of the crystal.

<sup>2</sup> Sproull, Dash, Tyler, and Moore, Rev. Sci. Instr. 22, 410 (1951).

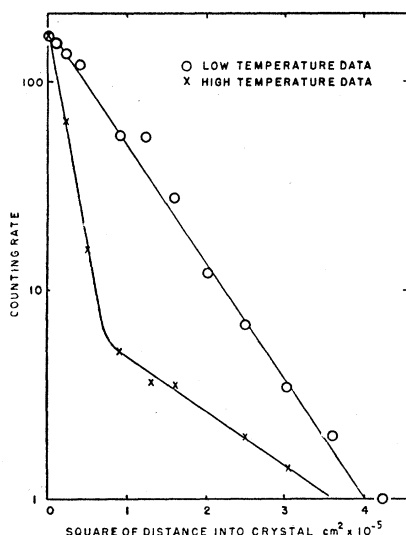


FIG. 2. The counting rate for a section plotted on a log scale against the square of the distance into the crystal at which the section was cut for a distribution obtained below 1350°K and for one obtained above 1350°K.

### III. INTERNAL DIFFUSION

The distribution predicted by a solution of the diffusion equation for a one-dimensional, semi-infinite solid with all the tracer material originally at the origin is

$$C = [Q/(\pi Dt)^{1/2}] \exp(-x^2/4Dt),$$

where  $C$  is the concentration,  $Q$  is the total amount of tracer material,  $D$  is the diffusion constant,  $x$  is the distance, and  $t$  is the time. The counting rate for a section is proportional to the concentration at approximately the center of the section, and thus a plot of the logarithm of the counting rate against the square of the distance should give a straight line with a slope of  $-(4Dt)^{-1}$ .

The internal diffusion results can be divided into two temperature ranges, a high temperature range from

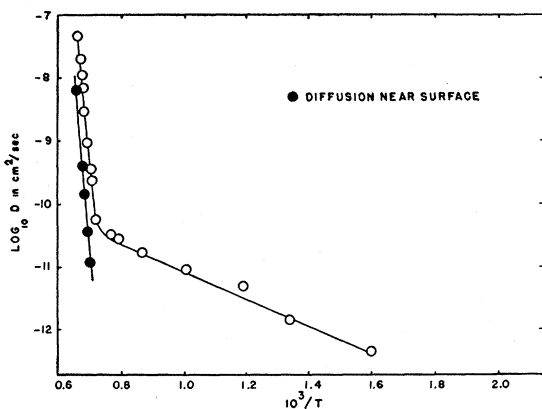


FIG. 3. The temperature dependence of the diffusion constants,  $\log D$  versus  $10^3/T$ . The open circles represent the non-charge-transporting diffusion and the filled circles the charge-transporting diffusion, which was determined from the distribution near the surface.

1350° to 1500°K and a low temperature range from 600° to 1350°K. Not only was the temperature dependence quite different in these two temperature ranges, but the distribution of radioactive Ba was also different. Samples of the two types of distribution are shown in Fig. 2. The low temperature distributions were as predicted, but the high temperature distributions were quite different. The high temperature distribution can be described by two terms of the above type. The quenched crystal results and the ionic mobility measurements show that two diffusion mechanisms were present, and the high temperature data were analyzed in terms of two diffusion constants. The larger diffusion constant (which describes the distribution deep in the crystal) was determined from the smaller slope in the high temperature curve in Fig. 2. The counting rates corresponding to this larger diffusion constant were

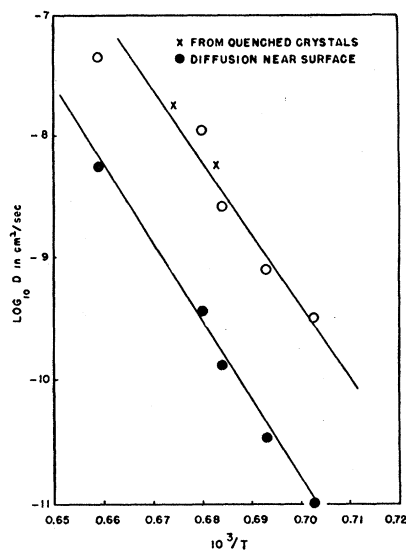


FIG. 4. The temperature dependence of the diffusion constants in the high temperature range. These are the same data as shown in Fig. 3, but plotted on an expanded scale.

subtracted from the counting rates near the surface, and the remainders were replotted on a  $\log C$  vs  $x^2$  graph. The smaller diffusion constant which described the distribution near the surface was calculated from the slopes of this plot. On the curves this smaller diffusion constant is referred to as "diffusion near surface."

The temperature dependence of the diffusion in these BaO crystals is shown in Figs. 3 and 4. Within the experimental error, the diffusion constants can be described by straight lines on these plots of  $\log D$  vs  $10^3/T$ . Thus the diffusion constants can be described by terms of the form

$$D = D_0 \exp(-E/KT).$$

The values of  $D_0$  and  $E$  for the various diffusion constants and temperature ranges are presented in Table I.

To investigate the "structure sensitive" low temperature range a series of measurements on the effects of

various heat treatments were made. The results are shown in Fig. 5. Most of the measurements were made at the same temperature, about 1150°K. These data were taken on samples cleaved from a different crystal than those used for the results in Fig. 3. The results of the internal diffusion measurements shown in Fig. 3 are replotted for comparison. An example of the difference in diffusion from crystal to crystal is shown by the measurement on the sample ("untreated crystal" on Fig. 5) which received the same treatment (i.e., mounting and polishing) as the previous crystals. This large variation was presumed to be caused by different impurity concentration. The quenched crystals showed the type of distribution found in the high temperature region with two diffusion constants. These are represented by the open and filled symbols on Fig. 5. The annealed crystal was heated to 1460°K and cooled at a slightly slower rate than that used in growing the crystals. This crystal showed the typical low temperature distribution. Two crystals were quenched simultaneously

TABLE I. Values of  $D_0$  and  $E$  for various diffusion constants and temperature ranges.  $D = D_0 \exp(-E/KT)$ .

Temperature range	Diffusion	$E$ ev	$D_0$ cm <sup>2</sup> /sec
High	"Deep in crystal"	11 ± 2.2	10 <sup>29±7</sup>
High	"Near the surface" (charged)	12 ± 2.3	10 <sup>31±8</sup>
Low	"Deep in crystal"	0.44 ± 0.03	10 <sup>-9±1a</sup>
Low—crystals quenched from 1460 deg K	"Deep in crystal"	0.5 ± 0.05	3 × 10 <sup>-6±1a</sup>
	"Near the surface" (charged)	0.3 ± 0.05	3 × 10 <sup>-10±1a</sup>
	Surface diffusion	0.16 ± 0.03	10 <sup>-6±1</sup>

\* Note: These values depend on the crystal used, and for the quenched crystals on the quenching temperature.

from 1460°K. One of these was measured at 1150°K and the other at a lower temperature to give an indication of the temperature dependence. From these data a "deep in the crystal" diffusion constant at 1460°K was calculated using the temperature dependence observed in the unquenched crystals, with the assumption that the defects were "frozen in" at the quenching temperature. A similar calculation was made for the crystal quenched from 1475°K. These two extrapolated points are the X's in Fig. 4. Because they agree with the measured values, they show that the "freezing in" temperature is very nearly the temperature from which they were quenched and that the number of defects in the quenched crystals is approximately the equilibrium number at the quenching temperature.

#### IV. IONIC MOBILITY

A series of measurements was made using quenched crystals and Ba electrodes<sup>3</sup> at 550°K. Three samples

<sup>3</sup> The initial measurements were made using platinum-rhodium electrodes. With unquenched crystals in the low temperature

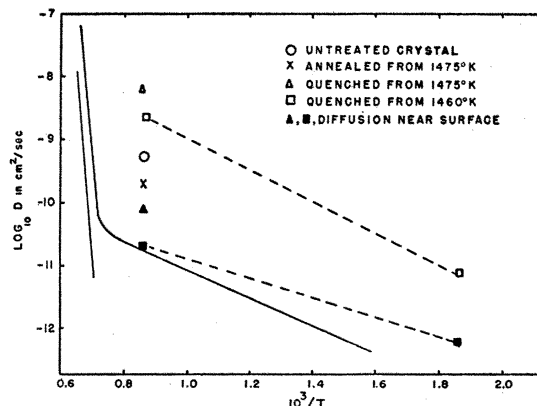


Fig. 5. The effects of heat treatment on the diffusion constants. The curves are replotted from Fig. 3, and the points are the diffusion constants in crystals receiving the treatment indicated in the key. The open symbols represent non-charge-transporting diffusion, and the filled symbols represent charge-transporting diffusion.

were cleaved from a crystal which had been quenched, and then ground and polished until it had two surfaces which were parallel within 0.001 radian. One was used with no field applied across the crystal. The other two were used with fields of 1100 v/cm and 3300 v/cm. The

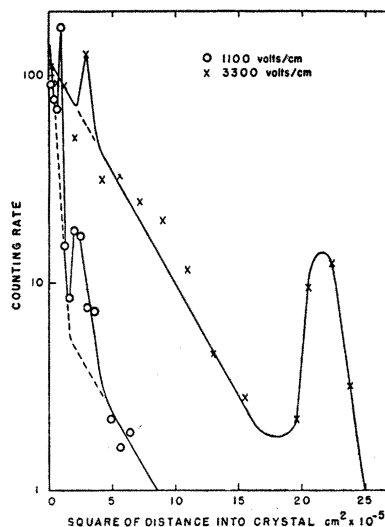


Fig. 6. The counting rate for a section plotted on a log scale against the square of the distance into the crystal at which the section was cut, for diffusion in the presence of the indicated dc electric fields, which were applied across the crystals in the plus  $x$  direction. The dotted portion of the curve at 1100 volts/cm was obtained from measurements with no applied field.

range, no difference was detected between diffusion with and against the field. A measurement in the high temperature range showed that the slower or "near the surface" diffusion transported approximately 2 electronic charges. Because the operating conditions were unstable at high temperatures, the measurements were continued on quenched crystals in the low temperature range. Measurements on these quenched crystals with the platinum-rhodium electrodes gave inconsistent results (probably caused by polarization of the crystal) of a few tenths of an electronic charge transported by the "near the surface" diffusion and no charge transported by the faster diffusion.

TABLE II. Data for three runs to measure ion mobility in the presence of an electric field.

Field volts/cm	$D$ cm <sup>2</sup> /sec ( $\times 10^{11}$ )	$E\mu t$ cm ( $\times 10^8$ )	Mobility, $\mu$ cm/sec volts/cm ( $\times 10^{10}$ )
—	$1.80 \pm 0.25$	—	—
$1100 \pm 20$	$1.83 \pm 0.50$	$4.75 \pm 0.25$	$5.76 \pm 0.40$
$3300 \pm 60$	$1.23 \pm 0.50$	$14.75 \pm 0.25$	$5.93 \pm 0.22$
Weighted averages	$1.71 \pm 0.25$		$5.89 \pm 0.22$
Average charge transported = $1.7 \pm 0.3$ electronic charges.			

results on these last two crystals are shown in Fig. 6. The dotted portions of the 1100 v/cm curve were calculated from the measurements with zero field. The first "peak" on each of the curves is caused by  $\text{La}^{140}$ , the radioactive daughter product of  $\text{Ba}^{140}$ ; this was learned from the decay of the counting rate of these samples. The second "peak" in each case is Ba. The data for a field of 1100 v/cm shows a high counting rate near the origin as if the electric field were not applied to part of the crystal, probably because of poor electrode contact over part of the surface.

The predicted distribution for charge transporting diffusion in the presence of an electric field for  $E\mu t \gg (4Dt)^{1/2}$  is approximately

$$C = [Q/(4\pi Dt)^{1/2}] \cdot [x/(x + E\mu t)] \exp[-(x - E\mu t)^2/4Dt],$$

where  $E$  is the field,  $\mu$  is the ionic mobility, and the other symbols have the same meaning as before. Thus the location of the peak is  $E\mu t$ , and the half-width of the peak gives a measure of the diffusion constant. This equation was obtained by solving

$$\partial C/\partial t = D(\partial^2 C/\partial x^2) - E\mu(\partial C/\partial x)$$

by Laplace transforms with a delta-function at the origin at  $t=0$  and with the concentration zero for negative  $x$  and approaching zero at  $x$  approaching  $\infty$ . The equation can be verified to order  $(4Dt)^{1/2}/E\mu t$  by differentiation. The form of the equation can be shown qualitatively by considering the case in which the medium is infinite in both directions. In this case a transformation to a coordinate system moving with a velocity  $E\mu$  gives the usual diffusion equation and immediately gives the exponential term. The additional terms in the above equation are caused by the asymmetry of a semi-infinite medium. The data for these three runs are shown in Table II. The charge transported by the diffusing barium was calculated with Einstein's relation:

$$\mu/D = q/kT.$$

The charge transported by the diffusing barium calculated from the average values was 1.7 electronic charges with an estimated probable error of 0.3 electronic charges. This was the charge transported by the slower or "near the surface" diffusion. As can be seen from Fig. 6, the slopes of the portions of the curves corre-

sponding to the faster diffusion are the same, independent of the field, which indicates that the faster diffusion was not affected by the field.

## V. SURFACE DIFFUSION

A measurement of the surface diffusion constant as a function of temperature was made, primarily to evaluate the possibility that the low temperature range internal diffusion was along cracks. All of these measurements were taken with low activity samples, which lead to a large random error in the measured distributions. Two types of initial distribution were used. For the three measurements in the middle of the temperature range investigated, the initial distribution was a band of radioactive Ba (as BaO) about  $\frac{1}{4}$  mm wide across a crystal surface. For the two measurements at the extremes of the temperature range, one-half the surface of a crystal was coated with tracer BaO. The distribution for the lowest temperature case is shown in Fig. 7. The temperature dependence of the surface diffusion is shown in Fig. 8. The two points which were taken with the microtome were the results of two ionic mobility measurements in which the edge surfaces of the crystal were not removed before sectioning the crystal. These two crystals showed a distribution far from ( $>10^{-2}$  cm) the front surface of the crystal, which was not present in another sample (cleaved from the same single crystal) which had been measured at about the same temperature and had had the edge surfaces removed before sectioning. This indicated that this portion of the distribution was probably on the surface and that the diffusion constant from this portion of the distribution was a surface diffusion constant. The values of  $D_0$  and  $E$  for the surface diffusion are given in Table I.

The estimated errors quoted in Table I are probable errors. These estimates were made from an evaluation of the scatter in the data and from an estimate of the probable error in the temperature measurement. The method used to estimate the error from the scatter in the data was a test for the significance of the slope of a

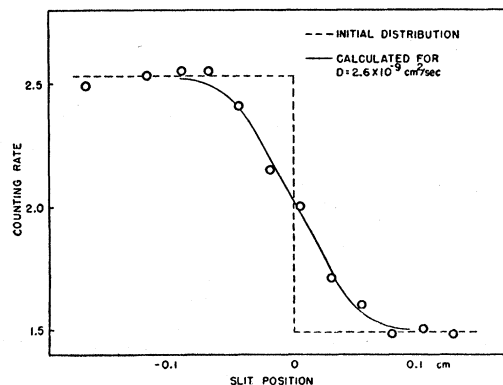


FIG. 7. Surface diffusion distribution of radioactive barium with a step function initial distribution.

regression line.<sup>4</sup> In making these estimates for the temperature dependence curves, the temperature was assumed to be correct, and the scatter was ascribed to the measurement of the diffusion constant. The random errors in the temperature measurement will affect the temperature dependence through their effect on the temperature range. This is the major source of error in the high temperature measurements. The probable error in the temperature measurement in the high temperature range was estimated from the heat transfer characteristics of the oven in the region around the crystal and thermocouple as  $\pm 20^\circ\text{C}$ . The thermocouple could not be in contact with the crystal because platinum reacts with barium oxide at high temperatures and this contributed to the uncertainty in the temperature. The oven power was monitored and no variations from a smooth curve of oven temperature against oven power were noted which were larger than the  $\pm 2$  percent accuracy of the power measurement. With such an unexpectedly large temperature dependence, it might be suspected that the higher measured temperatures were too low. A calculation of the rate of evaporation of one of the nickel leads to the oven winding showed that, if the actual temperature were about  $50^\circ\text{C}$  higher than the measured temperature, an easily detectable change in diameter would have occurred during the course of the runs at the higher temperatures. No such change was observed. The crystal was shielded from this nickel vapor (see Fig. 1).

An estimate of the expected standard deviation for the temperature dependence curves was made for two runs (one from each temperature range). These estimates agreed within a few percent with the estimates from the temperature dependence data, which indicates that the estimate of the temperature error is probably conservative.

## VI. DISCUSSION

Before these activation energies can be interpreted, some conclusions about the diffusion mechanism are necessary. The experimental observations indicate that two types of defects are required, one charge transporting and the other not. The numbers of both types of defects should vary reversibly with temperature in the high temperature range and it should be possible to "freeze in" both types of defects by quenching. The defect responsible for the non-charge-transporting diffusion process should be affected by impurities. The sharpness of the break in the typical high temperature curve shown in Fig. 2 indicates that the two diffusion mechanisms are substantially independent.

Four types of defects seem possible.<sup>5</sup> These are:

<sup>4</sup> Harold Cramer, *Mathematical Methods of Statistics* (Princeton University Press, Princeton, 1946), p. 548 ff.

<sup>5</sup> This smaller coupling between the two mechanisms suggests some type of linear or laminar defect in which a portion of the crystal has a larger diffusion constant than the rest. If the diffusing barium is assumed to spend almost all of its time in such a defect, the different temperature dependences in the two temperature ranges would be difficult to understand. The stronger

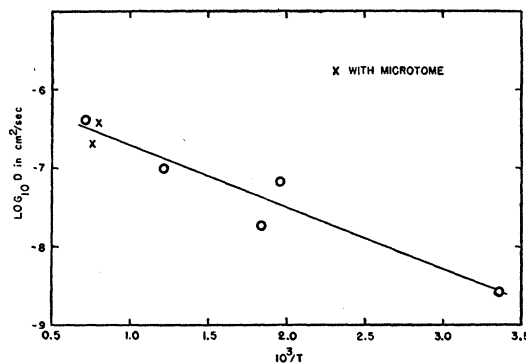


FIG. 8. Temperature dependence of the surface diffusion constant,  $\log D$  versus  $10^3/T$ .

bound pairs of barium and oxygen vacancies, interstitial Ba ions, Ba vacancies, and interstitial Ba atoms. The bound pairs of vacancies would presumably be insensitive to impurities. Moreover, bound pairs of vacancies would be expected to have lower activation energy for motion than either Ba vacancies or interstitial Ba ions. Calculations<sup>6</sup> of the activation energies of pairs of vacancies compared to dissociated vacancies for other ionic crystals support this conclusion. Since the opposite of these conclusions was observed in the quenched crystals, the bound pairs of vacancies can be eliminated.

This gives the tentative identification of the non-charge-transporting defect as interstitial Ba atoms. If the two types of defects were identified as interstitial barium atoms and ions, it would be difficult to understand why (1) the two diffusion mechanisms appear to be independent, and (2) quenching gives both charged and non-charged defects, but impurities only non-charged. This gives the tentative identification of the charge-transporting defect as Ba vacancies.

These two defects, Ba vacancies and interstitial Ba atoms, satisfy the observed characteristics with the possible exception of the small coupling between the two diffusion mechanisms. This point will be discussed in terms of a solution of an approximate equation for diffusion by interstitial atoms, as measured by radioactive tracer techniques.

The radioactive Ba was evaporated onto the crystal as a thin layer ( $\sim 10^{-4}$  cm thick) of BaO and thus did not introduce an appreciable or lasting gradient in the concentration of interstitial atoms. For an appreciable

temperature dependence in the high temperature range could not be ascribed to an increase in the number of these defects as this should affect the percentage of material diffusing by these defects as strongly as the rate of diffusion, contrary to the observations. If the temperature dependence in the high temperature range is interpreted in terms of barium diffusion through the lattice from defect to defect, a non-charge-transporting diffusion mechanism is still required through the lattice; otherwise the high temperature non-charge-transporting diffusion would have been affected by the electric field in the ionic mobility measurements. Thus, at most, these extended defects play a nonessential role and will not be further considered.

<sup>6</sup> G. J. Dienes, *J. Chem. Phys.* **16**, 620 (1948).

amount of this radioactive Ba to diffuse away by the interstitial atom mechanism, some interchange between the lattice ions and the interstitial atoms must take place. Furthermore, this interchange must be possible throughout the bulk of the material as well as in the evaporated layer. If radioactive Ba in an interstitial position in the evaporated surface layer could not interchange with a lattice ion in the interior of the crystal, an equilibrium between the radioactive ions in the surface layer and in interstitial positions only would result. Because the number of interstitial atoms is small, this would give a negligible transport of radioactive material away from the surface. At high temperatures this interchange could take place during the spontaneous formation and destruction of interstitial atoms. At low temperatures in the "structure sensitive" region some other mechanism is required. Presumably this interchange could take place as the interstitial atom passes between two lattice ions at the saddle point as it jumps from one interstice to the next. This process is not described by the usual diffusion equation. An approximate solution for this type of diffusion is given in the Appendix.

This solution indicates that distributions at the observed type could be obtained with a probability of interstitial atom-lattice ion interchange as small as  $10^{-10}$  per jump. The possibility of such a small probability of interchange is helpful in understanding the independence of the two diffusion mechanisms. For example, if this probability of interchange were  $10^{-8}$ , an interstitial atom would, on the average, take about  $10^8$  jumps or diffuse  $10^4$  atom spacings before interchange.

Qualitatively, the difference in magnitude of the two diffusion constants can be ascribed to the difference in the vibrational frequency of an interstitial Ba atom and a Ba ion adjacent to a Ba vacancy. These frequencies would have to differ by more than an order of magnitude. From the temperature dependence of the width of the  $F$ -center optical absorption band,<sup>7</sup> Klick<sup>8</sup> calculated the vibrational frequency of a potassium ion next to an  $F$  center in KCl as  $1.8 \times 10^{12}$ /sec. Comparison with the Reststrahlen frequency of  $4.8 \times 10^{12}$  gives a factor of approximately 3. The frequency of the interstitial atom would be expected to be higher than the normal lattice ion by a similar amount. Thus one might expect a factor of about 10 in an alkali halide and an even larger factor in BaO where the distortion around a defect should be even larger because of the large (34) dielectric constant.<sup>9</sup>

On the basis of the preceding discussion, the temperature dependence in the high temperature range can be interpreted in terms of the energy of formation of an interstitial Ba atom and a Ba vacancy. If  $W$  is the energy required to form such a pair and  $U$  is the activation energy for motion, the diffusion constants in the

high temperature range can be described by<sup>10</sup>

$$D = D_0 \exp(-(\frac{1}{2}W + U)/kT).$$

Using the data in Table I,  $W = 23 \pm 5$  ev.

Both the temperature dependence and the  $D_0$ 's for the high temperature range are unusually large. However, such large values are not unknown, since Seith<sup>11</sup> has found for the self-diffusion in bismuth perpendicular to the  $C$  axis a  $D_0$  of  $2.4 \times 10^{46}$  and a temperature dependence of 6.1 ev. Both empirical<sup>12</sup> and theoretical<sup>13</sup> correlations between  $D_0$  and the temperature dependence have been proposed. The large ( $\sim 10^{80}$ )  $D_0$ 's for the diffusion of Ba in BaO are consistent with these proposals.

## VII. CONCLUSIONS

Diffusion of Ba in BaO takes place by two mechanisms and defects are responsible for both. These defects have the following characteristics:

- (a) The number of defects responsible for both diffusion mechanisms vary reversibly with temperature above 1350°K.
- (b) The defects responsible for both processes can be "frozen in" by quenching.
- (c) The defects responsible for the neutral diffusion can be affected by impurities.

Of the five types of defects considered (barium vacancies, interstitial barium atoms, interstitial barium ions, bound pairs of barium, and oxygen vacancies, and a linear or laminar type defect), only the combination of the interstitial atom and the barium vacancy gave a phenomenologically correct account of the experimental observations. Furthermore, a simple theory of isotopic diffusion by interstitial atoms encounters no quantitative contradictions.

On the basis of this identification, the energy required to form an interstitial barium atom and a barium vacancy is  $23 \pm 5$  ev. The activation energy for motion of the interstitial barium atom is  $0.44 \pm 0.03$  ev, and for the motion of a barium vacancy  $0.3 \pm 0.05$  ev.

The charge transported by the barium vacancy is  $1.7 \pm 0.3$  electronic charges.

Although the temperature dependence of the surface diffusion ( $0.16 \pm 0.03$  ev) is not well established, the order of magnitude of the surface diffusion constant at temperatures around 1000°K is about  $10^{-7}$  cm<sup>2</sup>/sec. A comparison of this value with the internal diffusion constants in this temperature range indicates that, in agglomerations of particles (such as oxide cathodes) of less than  $0.2 \mu$  diameter, surface diffusion can be expected to be the predominate diffusion process.

The following qualitative conclusions can be drawn from a comparison of the ionic mobility measurements with the electronic conductivity measurements.<sup>14</sup>

<sup>10</sup> N. F. Mott and R. W. Gurney, *Electronic Processes in Ionic Crystals* (Clarendon Press, Oxford, 1948), p. 34.

<sup>11</sup> W. Seith, *Z. Electrochemie* **39**, 538 (1933).

<sup>12</sup> G. J. Dienes, *J. Appl. Phys.* **21**, 1189 (1950).

<sup>13</sup> C. Zener, *J. Appl. Phys.* **22**, 372 (1951).

<sup>14</sup> R. L. Sproull and W. W. Tyler, *Semi-Conducting Materials* (Butterworths, London, 1951), pp. 112-131.

<sup>7</sup> E. Burstein and J. J. Oberly, *Phys. Rev.* **78**, 349 (1950).

<sup>8</sup> C. C. Klick, *J. Opt. Soc. Am.* **41**, 816 (1951).

<sup>9</sup> R. S. Bever and R. L. Sproull, *Phys. Rev.* **83**, 801 (1951).

In the temperature range from 500 to 1350°K, the ionic conductivity in the untreated crystals is negligible compared with the electronic conductivity, but could easily be the order of a few percent in quenched crystals or in crystals with a different type of impurity.

Because the temperature dependence of the charge-transporting diffusion process in the low temperature range is about half that for the electronic conductivity, the ionic conductivity might dominate at room temperature and below.

Because of the very rapid increase with temperature above 1350°K, the ionic conductivity should be important at temperatures above this.

The author is greatly indebted to Professor R. L. Sproull for advice and assistance in this work and to Professor J. A. Krumhansl for many discussions.

#### APPENDIX

Let  $C$  be the concentration of barium,  $C_i$  be the concentration of barium in interstitial positions, and  $C_0$  be the concentration of barium in lattice positions, and let an \* indicate radioactive concentrations. Then,

$$C^* = C_0^* + C_i^*, \quad (1)$$

and

$$dC^*/dt = dC_0^*/dt + dC_i^*/dt. \quad (2)$$

Let the probability of an interstitial atom-lattice ion interchange per jump be  $p$ , and let  $q_i$  be the probability per second of jumping. There are two contributions to  $dC_0^*/dt$ :  $pq_i C_i^*$ , the number of radioactive interstitial atoms which become lattice ions per unit time; and  $-pq_i C_i C_0^*/C_0$ , the number of radioactive ions which become interstitial atoms per unit time. There is no contribution to  $dC_0^*/dt$  from the gradient of  $C_0^*$  in the simplest case in which no other diffusion mechanism is present.

There are three terms that contribute to  $dC_i^*/dt$ . The first two are the same as above, but with opposite sign. The third term is the contribution from the flow of radioactive interstitial atoms due to the isotopic gradient. This can be written as

$$\beta_i q_i a^2 (1-p) d^2 C_i^*/dx^2,$$

where  $\beta_i$  is a geometrical factor which gives the probability that an interstitial atom jumps in a particular direction, and  $a$  is the lattice spacing. The factor  $(1-p)$  is the probability that it jumps without interchanging. Thus

$$dC^*/dt = \beta_i q_i a^2 (1-p) d^2 C_i^*/dx^2. \quad (3)$$

The equation

$$dC_0^*/dt = -pq_i C_i C_0^*/C_0 + pq_i C_i^*$$

can be rewritten as

$$dC^*/dt + pq_i C_i C^*/C_0 = pq_i (1 + C_i/C_0) C_i^* + dC_i^*/dt.$$

Let  $A = pq_i C_i/C_0$  and  $B = pq_i (1 + C_i/C_0)$ . Then

$$C_i^* = \exp(-Bt) \int^t [dC^*(x, t')/dt' + AC^*(x, t')] \times \exp(Bt') dt', \quad (4)$$

$$= C^* - pq_i \exp(-Bt) \int^t C^*(x, t') \exp(Bt') dt'. \quad (5)$$

If  $C^*(x, t')$  is assumed to be approximately constant for  $t-t' \sim 1/B$  and  $C^*(x, t')$  is expanded by Taylor's series in terms of  $t-t'$ , the first two terms give

$$\begin{aligned} C_i^* &= C^* - C^*/(1 + C_i/C_0) \\ &\quad + (dC^*/dt) / [pq_i (1 + C_i/C_0)^2], \quad (6) \\ &\doteq C_i C^*/C_0 + (dC^*/dt) / pq_i. \end{aligned}$$

The quantity  $B$  is approximately equal to the probability of interchange per second per interstitial atom. Thus this assumption restricts us to the case in which the concentration is varying slowly with respect to the rate of interchange, and the distribution of radioactive Ba between lattice sites and interstices is almost the equilibrium distribution. This condition will be satisfied if the probability of interchange is large enough. Inserting this in Eq. (3) gives

$$dC^*/dt = \beta_i q_i a^2 (1-p) (C_i/C_0) (d^2/dx^2) \times [C^* + (C_0/pq_i C_i) dC^*/dt] \quad (7)$$

or

$$\begin{aligned} &= \beta_i q_i a^2 (1-p) (C_i/C_0) (d^2/dx^2) \\ &\quad \times [C^* + \beta_i a^2 \{(1-p)/p\} d^2 C^*/dx^2]. \end{aligned}$$

The observed distributions can be described as

$$C^* = C_0 \exp(-x^2/4DT), \quad (8)$$

which is a solution of the ordinary diffusion equation

$$dC^*/dt = D d^2 C^*/dx^2. \quad (9)$$

Thus  $\beta_i q_i a^2 (1-p) C_i/C_0$  can be identified as the diffusion constant if

$$\beta_i a^2 [(1-p)/p] d^2 C^*/dx^2 \ll C^*.$$

From (9),  $d^2 C^*/dx^2 = (x^2/4D^2 t^2 - 1/2Dt) C^*$ , and thus for the approximations to be valid,

$$\beta_i a^2 [(1-p)/p] (x^2/4D^2 t^2 - 1/2Dt) \ll 1.$$

With  $\beta_i = 1/6$ ,  $a = 2.8 \times 10^{-8}$  cm,  $x \sim 10^{-2}$  cm, and  $Dt \sim 10^{-5}$  for the last 9/10 of a run, the inequality is satisfied for  $p > 10^{-10}$  interchanges per jump. The order of magnitude of  $q_i$ , the jump frequency, can be estimated as  $10^{10}$ , which, with  $p \sim 10^{-10}$ , indicates that  $B$ , the probability of interchange, is greater than 1 per second. Thus, the approximate solution should be valid for the present case. Qualitatively, the effect of a smaller  $p$  on the distribution would be a curvature in the plot of the logarithm of the counting rate versus the square of the distance into the crystal. Within the experimental error, no such curvature was noticed.